Identification of molecular regulation on difference of lipid deposition in dedifferentiated preadipocytes from different chicken tissues

zheng ma
Foshan University
Na Luo
Chinese Academy of Agricultural Sciences
Lu Liu
Chinese Academy of Agricultural Sciences
Huanxian Cui
Chinese Academy of Agricultural Sciences
Jing Li
Foshan University
Hai Xiang
Foshan University
Huimin Kang
Foshan University
Hua Li
Foshan University
Guiping Zhao (zhaoguiping@caas.cn)
Foshan University, Chinese Academy of Agricultural Sciences

Research article

Keywords: Dedifferentiated preadipocytes, Different tissue derivation, lipid deposition, DEGs, Chicken

Posted Date: January 14th, 2021

DOI: https://doi.org/10.21203/rs.3.rs-38220/v2

Version of Record: A version of this preprint was published at BMC Genomics on April 3rd, 2021. See the published version at https://doi.org/10.1186/s12864-021-07459-8.

Abstract

Background: The body distribution with high intramuscular fat and low abdominal fat is ideal goal for broiler breeding. Preadipocytes with different origins have differences in metabolism and gene expression. This transcriptome analysis of intramuscular preadipocytes (DIMPs) and adipose tissue-derived preadipocytes (DAFPs) is aim to explore the characteristics in lipid deposition of different chicken preadipocytes by dedifferentiation in vitro.

Results: Compared to DAFPs, the total lipid content was decreased (P <0.05) in DIMFPs after two days with 100% confluence. Moreover, 72 DEGs related to lipid metabolism were screened, which are involved in the adipocyte differentiation, fatty acid transport and fatty acid synthesis, lipid stabilization, and lipolysis. Among the 72 DEGs, 19 DEGs were enriched in the PPAR signaling pathway, indicating a main contribution to the regulation of the difference of lipid deposition between DAFPs and DIMFPs. Among these 19 genes, the representative *APOA1*, *ADIPOQ*, *FABP3*, *FABP4*, *FABP7*, *HMGCS2*, *LPL* and *RXRG* genes were down-regulated, but *ACSL1*, *FABP5*, *PCK2*, *PDPK1*, *PPARG*, *SCD*, *SCD5*, *SLC27A6* genes were up-regulated (P < 0.05 or P < 0.01) in the DIMFPs. In addition, the well-known pathways affecting lipid metabolism (MAPK-, TGF beta-, Calcium-, PPAR signaling pathway) and the pathways related to cell communication were enriched, which may also contribute to the regulation of lipid deposition. Finally, the regulatory network for the difference of lipid deposition between chicken DAFPs and DIMFPs were proposed based on the above information.

Conclusions: Our data suggested the difference of lipid deposition between DIMPs and DAFPs of chicken *in vitro*, and proposed the molecular regulatory network for the difference of lipid deposition between chicken DAFPs and DIMFPs. The lipid content was significantly increased in DAFPs by the direct mediation of PPAR signaling pathways. These findings provide new insights into the regulation of tissue-specific fat deposition and optimizing body fat distribution in broilers.

Background

Fat has unique distribution characteristics and different economic value in various tissues of animals. In broilers, high-intensity artificial breeding has effectively increased meat yield, but also increased abdominal fat content and reduced intramuscular fat deposition [1]. Excessive abdominal fat deposition has negative impacts on feed efficiency and carcass yield [2,3]. Decreased abdominal fat deposition is beneficial to reduce produces waste and improve consumer acceptance. In contrast, intramuscular fat is economically desirable in broiler production. Appropriately increased IMF content can improve meat quality, including color, tenderness, flavor and juiciness [4-7]. Lowering abdominal fat and increasing intramuscular fat can effectively increase the economic value of broilers.

Previous studies have showed that adipocytes with different origins exhibited differential differentiation capabilities [8]. Compare with subcutaneous preadipocytes, the cell size and lipid droplets in intramuscular adipocytes are smaller [9,10], and the gene expression and enzyme activation related to

lipid metabolism are lower in intramuscular adipocytes [11,12]. Similarly, abdominal fat-derived preadipocytes exhibited a higher adipogenic differentiation ability than intramuscular fat-derived preadipocytes in chickens [13,14]. However, it is still unknown whether the difference in the lipogenesis ability of preadipocytes from different tissues will disappear after cultivating in vitro.

In this study, we explored the characteristics in lipogenesis of chicken preadipocytes with different origins after cultivating in vitro, including the dedifferentiated intramuscular preadipocytes (DIMFPs) and the dedifferentiated abdominal preadipocytes (DAFPs). These results will help to understand tissue-specific lipid deposition and optimizing body fat distribution in broilers.

Results

Difference of lipid deposition in two-type preadipocytes

Without differentiation induction, the DIMFP and DAFP cells after 2 days with 100% confluence was simultaneously collected for the detection of contents of total lipid. As shown in Figure 1a, total lipid content in DAFP cells was significantly ($P < 0.05$) higher than that in DIMFP cells. The main ingredient of lipid, , triglyceride (TG), phospholipid (PLIP) and total cholesterol (TCHO) also were detected. Similarly, the TG content in DAFP cells was significantly ($P < 0.05$) higher than that in DIMFP cells. But the contents of PLIP and TCHO showed no difference in two types of preadipocytes (Figure 1b).

Identification of DEGs

Total RNA of each three cell repetitions of DIMFP and DAFP group were extracted for RNA-sequencing. A total of 21,469 expressed genes were found in DIMFPs and DAFPs (Additional file 1: Table S1). Using gene expression profiling and comparing the DAFP group with the DIMFP group (DIMFP vs DAFP), a total of 3629 known DEGs ($|\log2\ FC| \geq 0.5$, with $p < 0.05$) were screened (Figure 2a), of which, 2579 DEGs were down-regulated and 907 DEGs were up-regulated (Additional file 2: Table S2). Next, the cluster analysis was performed on these 21,469 genes, two results showed the same situation: three cell samples of the same groups were clustered together, respectively (Figure 2b).

Analysis of the enriched GO terms and pathways in two-type preadipocytes

Based on 3629 known DEGs, the Gene Ontology (GO) analysis were performed, and 56 GO terms were enriched ($P < 0.05$) and mainly included the following processes: cell adhesion, tight adhesion, cell differentiation, extracellular matrix, DNA binding, cacium ion binding, et al. (Additional file 3: Table S3), the top 10 terms of each of the biological process (BP), cellular component (CC) and molecular function (MF) were shown in Figure 3.

Meanwhile, 47 pathways were found to be significantly enriched (Corrected *P*-value < 0.05) (Additional file 4: Table S4), including some well-known pathways affecting lipid metabolism (PPAR- MAPK-, TGF beta-, Wnt-, Calcium signaling pathway) and other pathways related to cell communications (Focal adhesion, Cytokine-cytokine receptor interaction, ECM-receptor interaction, Tight junction, Regulation of

actin cytoskeleton, Cell adhesion molecules, Adherens junction). The top 15 enriched pathways were shown in Figure 4.

DEGs related to lipid metabolism in two-type preadipocytes

GO enrichment analysis indicated that 72 DEGs related to lipid metabolism, and some representative DEGs were screened (Additional file 5: Table S5). For the DEGs related to lipid metabolism, they mainly involved in the adipocyte differentiation (such as *CEBPA*, *PPARG*, *RBP7* and *RXRG*), fatty acid transport and fatty acid synthesis (such as *ELOVL1*, *ELOVL6*, *FABP3*, *FABP4*, *FADS6*, *FADS1L1*, *SCD* and *SCD5*), lipid stabilization (such as *CIDEC*, *PLIN3*, *PLIN4* and *MOGAT1*), and lipolysis (such as *DGKD*, *DGKH*, *DGKQ* and *LPL*). The 20 representative DEGs related to lipid metabolism were randomly selected to validate the gene expression profiling results by qRT-PCR, and the correlation of gene expression profiling and qRT-PCR were analyzed by Spearman rank correlation to confirm the accuracy of the data. The result showed that the fold change of gene expression between the two methods was significantly correlated (Figure 5a) ($r = 0.9666$, $P < 0.01$).

Among these 20 verified genes, the expression levels of *CEBPA*, *DGKH*, *DGKQ*, *DGKD*, *FADS1L1*, *SCD*, *SCD5* and *PPARG* were significantly ($P < 0.05$ or $P < 0.01$) downregulated in DAFPs compared to DIMFPs (Figure 5b). However, It was found that the expression of *CIDEC*, *ELOVL1*, *ELOVL6*, *FABP3*, *FABP4*, *FADS6*, *LPL*, *MOGAT1*, *PLIN3*, *PLIN4*, *RBP7* and *RXRG* genes were significantly (all $P < 0.01$) up-regulated in DAFPs compared to DIMFPs (Figure 5c).

Pathways involved in lipid metabolism

It was found that 19 genes related to lipid metabolism which enriched in the PPAR signaling pathway (Additional file 7: Figure S1). Among these 19 genes, the data from RNA-seq showed that *APOA1*, *ADIPOQ*, *FABP3*, *FABP4*, *FABP7*, *HMGCS2*, *LPL* and *RXRG* genes were down-regulated, but *ACSL1*, *FABP5*, *PCK2*, *PDPK1*, *PPARG*, *SCD*, *SCD5*, *SLC27A6* genes were up-regulated ($P < 0.05$ or $P < 0.01$) in the DIMFPs.(Additional file 2: Table S2).

Also, there are a large number of DEGs that were enriched in MAPK- (80 genes), Calcium- (50 genes), and TGF beta (30 genes) signaling pathway, which involved in mediating the biology function of lipid metabolism (Additional file 8: Figure S2, Additional file 9: Figure S3, and Additional file 10: Figure S4). In addition, 245 DEGs also were enriched the pathways related to cell communications (Focal adhesion, Cytokine-cytokine receptor interaction, ECM-receptor interaction, Tight junction, Regulation of actin cytoskeleton, Cell adhesion molecules, Adherens junction). However, it was found that the enriched Wnt signaling pathway, as a well-known pathway affecting lipid metabolism, did not medicate the regulation on lipid metabolism. Based on the above information, we proposed the regulatory network for the difference of lipid deposition between chicken DAFPs and DIMFPs (Figure 6).

Discussion

Fat has unique distribution characteristics and different economic value in various tissues of animals. In broilers, the intramuscular fat is economically desirable in production. Appropriately increased IMF content can improve meat quality, including tenderness, flavor and juiciness [4-6]. However, excessive abdominal fat deposition has negative impacts on feed efficiency and carcass yield [2,3], and decreased abdominal fat deposition is beneficial to reduce produces waste and improve consumer acceptance. Lowering abdominal fat and increasing intramuscular fat can effectively increase the economic value of broilers. Therefore, how to change the constitution distribution is an important scientific problem for broilers.

Unlike a marbling distribution of IMF in domestic animals, the IMF of chicken cannot be obtained directly from anatomy. Moreover, muscle tissue of chicken has a variety of cell composition [15], the preadipocytes of IMF can not be separated by physical methods for the similar density with muscle cells. So, the high purity preadipocytes of IMF can only be obtained by the dedifferentiation of mature adipocytes in vitro as described previously[16]. In this study, the abdominal fat preadipocytes and intramural preadipocytes were respectively obtained from the mature adipocytes of the same chicken to compare their lipogenesis ability with the consistency of experimental conditions *in vitro*, expecting to establish a theoretical foundation for the body fat distribution of chicken and provide ideas and development direction for chicken production.

As known, the adipocytes in different tissues were regulated by the adjacent microenvironment to perform the corresponding physiological function [17,18]. To eliminate the effect of factors in vivo and in vitro, the second-generation cells used. After the cells were overgrown for 2 days, the lipogenesis of adipocytes were detect, which was different from the usual practice of inducing adipocyte differentiation in vitro, avoiding the possibility that the inducers could conceal the lipogenesis of the cells themselves. The results showed that the lipogenesis of preadipocytes derived from abdominal adipocytes were significantly superior to those derived from muscle tissue, consistent with those results *in vivo* as previously reported [19, 20], and the increase of TG content was responsible for the improvement of total lipid.

In order to identify the regulatory mechanism of lipid deposition for the difference between DIMPs and DAFPs, the RNA-sequencing was performed to screen the functional genes and important pathways related to lipid deposition, and the quality control by cluster analysis and qRT-PCR indicated the reliability of RNA-sequencing data. Based on the screened 3629 DEGs, the GO terms and KEGG analysis were performed. There are 47 enriched pathways were screened, including the well-known pathways affecting lipid metabolism (MAPK-, TGF beta-, Wnt-, Calcium-, PPAR signaling pathway, and the pathways related to cell communication). Furthermore, we identified the DEGs related to lipid metabolism according to the enriched GO terms and signaling pathways. Among the 72 DEGs related to lipid metabolism, 19 genes were enriched in the PPAR signaling pathway with the classic mediation on lipid metabolism [34,35], and the enriched genes included the representative *ACSL1*, *APOA1*, *ADIPOQ*, *FABP3*, *FABP4*, *FABP5*, *FABP7*, *HMGCS2*, *LPL*, *PCK2*, *PDPK1*, *PPARG*, *RXRG*, *SCD*, *SCD5* and *SLC27A6*, etc., which had the important regulation on lipid metabolism [21-37]. Therfore, it was considered that these

genes and PPAR signaling pathway had the important effects *in vitro* on regulating the difference of lipid deposition between DIMPs and DAFPs of chicken.

It was reported that MAPK-, TGF beta-, Wnt-, and Calcium signaling pathways have the interaction with the PPAR pathway to regulate the lipid metabolism in the lipogenesis process, and there are a large number of genes were enriched in MAPK-, Calcium-, and TGF beta signaling pathways [38-40]. According to the enrichment information of these three signaling pathways in this study, the evidence pointed to these three pathways could mediate the biology function of cell differentiation or metabolism. Then, it was deduced that the MAPK-, Calcium-, and TGF beta signaling pathways also involved the regulation of lipogenesis between DAFPs and DIMFPs. As our previous reported [41], these pathways related to cell communication also would participate in the regulation on the lipid deposition through MAPK signaling pathway in chicken. In this study, multiple enriched pathways related to cell communication were screened, inlcuding Focal adhesion, Cytokine-cytokine receptor interaction, Regulation of actin cytoskeleton, Tight junction, ECM-receptor interaction, Cell adhesion molecules (CAMs), suggesting the pathways related to cell communication had the effect on the difference of lipid deposition between DIMPs and DAFPs of chicken.

Conclusions

In brief, our data suggest that the difference of lipid deposition between DIMPs and DAFPs of chicken *in vitro*, and propose the molecular regulatory network for the difference of lipid deposition between chicken DAFPs and DIMFPs. The lipid content was significantly increased in DAFPs by the direct mediation of PPAR signaling pathways. These findings establish the groundwork and provide new insights into the regulation of tissue-specific fat deposition and optimizing body fat distribution in broilers. In the future, additional studies will be required to complement the effects of these important genes on lipid deposition and pathways in DIMPs and DAFPs.

Methods

Animals and Ethics Statement

Three BJY chickens were obtained from the Institute of Animal Sciences, CAAS (Beijing, China), which were raised under the same recommended environmental and nutritional conditions. Animal experiments were approved by the Science Research Department (in charge of animal welfare issues) at the Institute of Animal Sciences, Chinese Academy of Agricultural Sciences (CAAS) (Beijing, China). Three birds were individually euthanized by carbon dioxide anesthesia and exsanguination by severing the carotid artery at 10 days of age, the pectoralis major and abdominal fat tissues were excised to use the cell isolation.

Preadipocyte acquisition

The mature adipocytes from the pectoralis major and abdominal fat tissue were respectively isolated as previous method, and then the preadipocytes were obtained with the dedifferentiation treatment as

previous method [16]. The main protocol as follows:

The abdominal fat tissue and pectoralis major of three chickens were collected, and then washed with phosphate-buffered saline (PBS) containing 1% penicillin- streptomycin (Gibco, Thermo Fisher Scientific Inc., Shang hai, China). The abdominal fat tissue and pectoralis major from the same chicken were recorded for the one-to-one correspondence of cell samples in subsequent experiments. After removal of the blood vessels and connective tissue, the samples were finely minced to 1 mm3 with scissors, and then digested in DMEM/F12(1:1) medium (Gibco, Thermo Fisher Scientific Inc., Shang hai, China) contained 0.1% Type I collagenase (Sigma-Aldrich, Shanghai, China) in a water bath with continuous shaking at 37°C for 60 min. After terminated digestion and filtered, the cell suspension was centrifuged with 600 g for 15 min. The top layer containing mature adipocytes was collected and placed to a 25 cm^2 cell culture flask, which was inverted and completely filled with DMEM/F12(1:1) medium containing 10% FBS. The floating mature adipocytes would adhere to the bottom of the flask incubate in a 37°C incubator with 5% CO_2. After 3 days, the mature adipocytes would gradually converse to preadipocytes by releasing the lipid by exocytosis, and the medium was replaced and the flask was re-inverted so that the preadipocytes were on the bottom to proliferate massively. Up to 15 days, the confluence of preadipocytes would reach 80%-90%, cells were sub-cultured.

Preadipocytes culture and treatment

The medium was changed every 3 days. After reaching 80 % confluence, cells were passaged, and the second passage (P2) preadipocytes by the dedifferentiation of mature adipocytes from the pectoralis major (DIMFP) and abdominal fat tissue (DAFP) were used for further experiments. Both of DIMFP and DAFP were respectively plated in 24-well or 100-mm dishes, and cells were collected after 2 days with 100 % confluence for further RNA extraction and Measurement of biochemical indices (in 100-mm dishes), or Oil-red-O staining assay (in 24-well) .

Oil-red-O staining assay

The cellular lipid content of DIMFP and DAFP in 24-well were determined by oil-red-O staining. Staining procedure was conducted as follows: cell medium was discarded, washed 3 times with PBS, and then fixed with 4% formalin for 30 min. After fixed, the cells were washed 3 times with PBS and stained with oil-red-O (WuHan AmyJet Scientific Inc., Wuhan, China) for 60 min. Subsequently, the oil-red-O was discarded and washed 3 times. After water evaporated, isopropanol was added to extract the oil-red-O for 10 min, and then the absorbance values of the solutions were measured by the Varioskan™ LUX Multimode Microplate Reader (Thermo Fisher Scientific Inc., Shang hai, China) at 510 nm.

Measurement of biochemical indices

The TG, TCHO and PLIP contents in cell samples were measured using TG (Nanjing Jiancheng Bioengineering Institute, Nanjing, China), TCHO (Nanjing Jiancheng Bioengineering Institute, Nanjing, China) and PLIP (Beijing Lidemann Biochemical Co. , Ltd. , Beijing, China) assay kits. Cell samples from

each group were homogenized with absolute ethanol at room temperature and centrifuged (1000×g, 20 min). After centrifugation, the supernatant was used for TG, TCHO and PLIP measurement, respectively. The assay was performed according to the manufacturer's instructions.

RNA Extraction and Identification

Total RNA was extracted from DIMFP and DAFP in 100-mm dishes, using the Trizol reagent (Invitrogen, Carlsbad, CA, USA) according to the manufacturer's instructions. The quality of RNA was detected by 1.5% gel electrophoresis, and RNA concentration was determined by NANODROP2000 spectrophotometer (Thermo Fisher Scientific Inc., Shang hai, China). The OD260/280 values of all samples were limited to the range of 1.8 to 2.0. The RNA samples were subsequently used for gene expression profiling.

Gene Expression Profiling

Based on ultra-high-throughput sequencing (HiSeq2500; Illumina, San Diego, CA, USA), gene expression profiling was undertaken by Berry Genomics (Beijing, China). Raw data were converted to FASTQ files using bcl2fastq (Illumina). Clean reads were generated by removing reads with adapter and low-quality sequences and mapped to the reference chicken genome and genes (Gallus gallus, Galgal6; available at https://www.ncbi.nlm.nih.gov/assembly/GCF_000002315.6) using TopHat 1.3.2 (https://ccb.jhu.edu/software/tophat). Gene expression levels were calculated using the RPKM method, as described by Mortazavi et al [42]. Differentially expressed genes (DEGs) between the DIMFP and DAFP were analyzed using the edgeR R package. DEGs were screened by the following criteria: $|\log_2 FC| \geq 1.0$, with FDR < 0.05. Based on the DEGs, clustering analysis was performed in each sample by the pheatmap package of R software. Hierarchical clustering was performed on both rows and columns, and the resulting dendrogram was saved as an image file.

Gene Ontology and Kyoto Encyclopedia of Genes and Genomes Analysis

Gene Ontology (GO) enrichment analysis was performed to identify the gene function classes and categories corresponding to the DEGs using the ClueGO plug-in and CluePedia plugin of Cytoscape (https://cytoscape.org/). The significance level of GO terms enrichment was set at $P < 0.05$ as indicated. According to the results of GO enrichment analysis, DEGs related to abdominal adipose tissue metabolism were screened. The significantly enriched signaling pathways of DEGs were analyzed by the Kyoto Encyclopedia of Genes and Genomes (KEGG) [43]. $P < 0.05$ was considered to be indicative of statistical significance.

Real-time quantitative polymerase chain reaction

Using the same RNA samples, real-time quantitative polymerase chain reaction (qRT-PCR) was performed to confirm the results of gene expression profiling. RNA samples were reverse transcribed using TIANGEN® FastQuant RT Kit (Tiangen, Beijing, China), and specific primers were designed placing at or

just outside of exon/exon junctions using Primer 5.0 software dependent on GeneBank sequences (Additional file 6:Table S6).

Samples were amplified using the real-time PCR Detection System ABI 7500 (Applied Biosystems, Carlsbad, California, USA). The PCR mixture contained 10 μL of 2 × iQ™ SYBR Green Supermix, 0.5 μL (10 mmol) of each primer, and 1 μL of cDNA, along with ddH_2O for a total volume of 20 μL. After initial denaturation for 30 s at 95 °C, amplification was performed for 40 cycles (95 °C for 5 s and 60 °C for 32 s). The actin beta (β-actin) expressions were used as the normalization control by the $2^{-\triangle\triangle Ct}$ method to determine fold-changes in gene expression [44]. A melting curve was constructed to verify the single amplified PCR product. Samples were assayed in triplicate, with standard deviations of cycle threshold values did not exceed 0.5 on a within-run basis. Correlations between relative abundance from qRT-PCR and gene expression profiling data were also calculated.

Statistical analysis

Three comparison replicates (DIMFP vs DAFP) of the cell experiment were set according to the one-to-one correspondence of cell samples from the abdominal fat tissue and pectoralis major of the same chicken. All data are presented as the means ± SEM, for three replicates of the experiment. Statistically significant differences between the two culture conditions were tested by independent-samples t-tests using SAS 9.2 software. $P < 0.05$ (*) or $P < 0.01$ (**) was considered to be significant. All figures were constructed using GraphPad Prism version 5.02 (GraphPad Software Inc, La Jolla, CA).

Abbreviations

ACSL1: Acyl-CoA synthetase long-chain family member 1; APOA1: Apolipoprotein A1; ADIPOQ: Adiponectin, C1Q and collagen domain containing; BP: Biological Process; CC: Cellular component; CEBP: CCAAT enhancer binding protein; CIDEC: Cell death inducing DFFA like effector c; DEG: Differentially expressed genes; DIMFPs: Dedifferentiated intramuscular preadipocytes; DAFPs: Dedifferentiated abdominal preadipocytes; DGK: Diacylglycerol kinase; ELOVL: Elongase of very long-chain fatty acids-like; FABP: Fatty acid binding protein; FADS: Fatty acid desaturase; HMGCS2: 3-hydroxy-3-methylglutaryl-Coenzyme A synthase 2; IMF: Intramuscular fat; GO: Gene Ontology; KEGG: Kyoto Encyclopedia of Genes and Genomes; LPL: Lipoprotein lipase; MAPK: Mitogen- activated protein kinase; MF: Molecular Function; MOGAT: Monoacylglycerol O-acyltransferase; PBS: Phosphate-buffered saline; PCK2: Phosphoenolpyruvate Carboxykinase 2; PDPK1:3-phosphoinositide dependent protein kinase-1; PLIN: Perilipin; PPAR: Peroxisome proliferators-activated receptors; qRT-PCR: Quantitative Real-time Polymerase Chain Reaction; RBP: Retinol binding protein; RXR: Retinoid X receptor; SCD: Stearoyl-CoA desaturase; Wnt: Wingless/Int.

Declarations

Acknowledgements

Not applicable.

Authors' contributions

ZM and NL performed the study, analyzed the data, and drafted the manuscript. JL performed the study. LL drafted the manuscript. HXC, HX and HMK contributed to the design of the study, and modifying the manuscript. GPZ and LH designed the study and was in charge of the overall project. All authors submitted comments on drafts, and read and approved the final manuscript.

Funding

The research was funded by grants from the High level talent program of Foshan University (No. cgz07243), Key-Area Research and Development Program of Guangdong Province (No. 2020B020222002), Innovation Team of Precise Animal Breeding (No. 2019KCXTD004) and Guangdong Provincial Key Laboratory of Animal Molecular Design and Precise Breeding (No. 2019B030301010, No. 201KSYS011). The funding agencies had not involved in the experimental design, analysis and interpretation of the data or writing of the manuscript.

Availability of data and materials

All the data obtained in the current study have been presented in this article. The RNA-Seq sequence raw data-set supporting the results of this study have been deposited at the National Center for Biotechnology Information (NCBI).

Ethics approval and consent to participate

This study was conducted in accordance with the Guidelines for Experimental Animals established by the Ministry of Science and Technology (Beijing, China). All experimental protocols were approved by the Science Research Department (in charge of animal welfare) of the Institute of Animal Sciences, Chinese Academy of Agricultural Sciences (CAAS), Beijing, China.

Consent for publication

Not applicable.

Competing interests

The authors declare that they have no competing interests.

References

1. Ma JS, Chang WH, Liu GH, Zhang S, Zheng AJ, Li Y, et al. Effects of Flavones of Sea Buckthorn Fruits on Growth Performance, Carcass Quality, Fat Deposition and Lipometabolism for Broilers. Poult Sci. 2015 ; 94(11):2641-2649.

2. Demeure O, Duclos MJ, Bacciu N, Le Mignon G, Filangi O, Pitel F, et al. Genome-wide interval mapping using SNPs identifies new QTL for growth, body composition and several physiological variables in an F2 intercross between fat and lean chicken lines. Genetics Selection Evolution. 2013; 45:36.
3. Ramiah SK, Meng GY, Sheau WT, Swee KY, Ebrahimi M. Dietary Conjugated Linoleic Acid Supplementation Leads to Downregulation of PPAR Transcription in Broiler Chickens and Reduction of Adipocyte Cellularity. PPAR Research. 2014; 2014:137652.
4. Nishimura The role of intramuscular connective tissue in meat texture. Anim Sci J. 2010; 81(1):21-27.
5. Ge K, Ye P, Yang L, Kuang J, Chen X, Geng Z. Comparison of slaughter performance, meat traits, serum lipid parameters and fat tissue between Chaohu ducks with high- and low-intramuscular fat content. Anim Biotechnol. 2019; 1-11.
6. FrankD, Watkins P, Ball A, Krishnamurthy R, Piyasiri U, Sewell J, et al. Impact of brassica and lucerne finishing feeds and intramuscular fat on lamb eating quality and f A cross-cultural study using Chinese and Non-Chinese Australian consumers. J Agric Food Chem. 2016; 64(36):6856-6868.
7. Starkey CP, Geesink GH, Collins D, Hutton Oddy V, Hopkins DL. Do sarcomere length, collagen content, pH, intramuscular fat and desmin degradation explain variation in the tenderness of three ovine muscles? Meat Sci. 2016; 113:51-58.
8. Chu W, Wei W, Han H, Gao Y, Liu K, Tian Y, et al. Muscle-specific downregulation of GR levels inhibits adipogenesis in porcine intramuscular adipocyte tissue. Sci Rep. 2017; 7(1):510.
9. Kouba M, Bonneau M, 2009. Compared development of intermuscular and subcutaneous fat in carcass and primal cuts of growing pigs from 30 to 140kg body weight. Meat Sci, 81(1):270-274.
10. Arrighi N, Moratal C, Clément N, Giorgetti-Peraldi S, Peraldi P, Loubat A, et al. Characterization of adipocytes derived from fibro/adipogenic progenitors resident in human skeletal muscle. Cell Death Dis. 2015; 6(4):e1733.
11. Jiang S, Wei H, Song T, Yang Y, Peng J, Jiang S. Transcriptome comparison between porcine subcutaneous and intramuscular stromal vascular cells during adipogenic differentiation. PLoS One. 2013; 8(10):e77094.
12. Wang S, Zhou G, Shu G, Wang L, Zhu X, Gao P, et al. Glucose utilization, lipid metabolism and BMP-Smad signaling pathway of porcine intramuscular preadipocytes compared with subcutaneous preadipocytes. Cell Physiol Biochem. 2013; 31(6):981-996.
13. Hausman GJ, Poulos S. Recruitment and differentiation of intramuscular preadipocytes in stromal-vascular cell cultures derived from neonatal pig semitendinosus muscles. J Anim Sci. 2004; 82(2):429-437.
14. Zhang M, Li F, Ma XF, Li WT, Jiang RR, Han RL, et al. Identification of Differentially Expressed Genes and Pathways Between Intramuscular and Abdominal Fat-Derived Preadipocyte Differentiation of Chickens in Vitro. BMC Genomics. 2019; 20(1):743.
15. Hocquette JF, Gondret F, Baeza E, Medale F, Jurie C, Pethick DW. Intramuscular fat content in meat-producing animals: development, genetic and nutritional control, and identification of putative

markers. Animal. 2010; 4:303–319.

16. Cui HX, Guo LP, Zhao , Liu RR, Li Method Using a Co-Culture System With High-Purity Intramuscular Preadipocytes and Satellite Cells From Chicken Pectoralis Major Muscle. Poult Sci. 2018; 97(10):3691-3697.
17. Zhou G, Wang S, Wang Z, Zhu X, Shu G, Liao W, Yu K, Gao P, Xi Q, Wang XJ. Global comparison of gene expression profiles between intramuscular and subcutaneous adipocytes of neonatal landrace pig using microarray. Meat Sci. 2010;86(2):440–50.
18. Sun WX, Wang HH, Jiang BC, Zhao YY, Xie ZR, Xiong K, Chen J. Global comparison of gene expression between subcutaneous and intramuscular adipose tissue of mature Erhualian pig. Genet Mol Res. 2013;12(4):5085–5101.
19. Mérida I, Ávila-Flores A, Merino E. Diacylglycerol kinases: at the hub of cell signalling. Biochem J. 2008; 409(1):1-18.
20. Sakane F, Mizuno S, Takahashi D, Sakai H. Where do substrates of diacylglycerol kinases come from Diacylglycerol kinases utilize diacylglycerol species supplied from phosphatidy-linositol turnover-independent pathways. Adv Biol Regul. 2018; 67:101-108.
21. Lefterova MI, Haakonsson AK, Lazar MA, Mandrup S. PPARγ and the global map of adipogenesis and beyond. Trends Endocrinol Metab. 2014; 25(6):293- 302.
22. Capobianco E, Martínez N, Fornes D, Higa R, Di Marco I, Basualdo MN, et al. PPAR activation as a regulator of lipid metabolism, nitric oxide production and lipid peroxidation in the placenta from type 2 diabetic patients. Mol Cell Endocrinol. 2013; 377(1-2):7-15.
23. Weihua Tian, Dandan Wang, Zhang Wang, Keren Jiang, Zhuanjian Li, Yadong Tian, et al. Evolution, expression profile, and regulatory characteristics of ACSL gene family in chicken (Gallus gallus). Gene. 2021; 764:145094.22.
24. Cryer A. Tissue lipoprotein lipase activity and its action in lipoprotein metabolism. Int J Biochem. 1981; 13:525–541.
25. Identification of differentially expressed genes and pathways between intramuscular and abdominal fat-derived preadipocyte differentiation of chickens in vitro
26. Meng Zhang, Fang Li, XiangFei Ma, WenTing Li, RuiRui Jiang, RuiLi Han, et al. Identification of differentially expressed genes and pathways between intramuscular and abdominal fat-derived preadipocyte differentiation of chickens in vitro. BMC Genomics. 2019; 20(1):743.
27. Mihelic R, Winter H, Powers JB, Das S, Lamour K, Campagna SR, et al. Genes controlling polyunsaturated fatty acid synthesis are developmentally regulated in broiler chicks. Br Poult Sci. 2020.
28. Wu X, Zou X, Chang Q, Zhang Y, Li Y, Zhang L, et al. The evolutionary pattern and the regulation of stearoyl-CoA desaturase genes. Biomed Res Int. 2013; 2013:856521.
29. Hughes AL, Piontkivska H. Evolutionary diversification of the avian fatty acid-binding proteins. Gene. 2011; 490(1-2):1-5.

30. Jin S, Lee SH, Lee DH, Manjula P, Lee SH, Lee JH. Genetic association of DEGS1, ELOVL6, FABP3, FABP4, FASN and SCD genes with fatty acid composition in breast and thigh muscles of Korean native chicken. Anim Genet. 2020; 51(2):344-345.
31. Li J, Xing S, Zhao G, Zheng M, Yang X, Sun J, et al. Identification of diverse cell populations in skeletal muscles and biomarkers for intramuscular fat of chicken by single-cell RNA sequencing. BMC Genomics. 2020; 21(1):752.
32. Liu L, Liu X, Cui H, Liu R, Zhao G, Wen J. Transcriptional insights into key genes and pathways controlling muscle lipid metabolism in broiler chickens. BMC Genomics. 2019; 20(1):863.
33. Nafikov RA, Schoonmaker JP, Korn KT, Noack K, Garrick DJ, Koehler KJ, et al. Association of polymorphisms in solute carrier family 27, isoform A6 (SLC27A6) and fatty acid-binding protein-3 and fatty acid-binding protein-4 (FABP3 and FABP4) with fatty acid composition of bovine milk. J Dairy Sci. 2013; 96(9):6007-6021.
34. Lee YE, He HL, Shiue YL, Lee SW, Lin LC, Wu TF, et al. The prognostic impact of lipid biosynthesis-associated markers, HSD17B2 and HMGCS2, in rectal cancer treated with neoadjuvant concurrent chemoradiotherapy. Tumour Biol. 2015; 36(10):7675-7683.
35. Pazhouhandeh M, Sahraian MA, Siadat SD, Fateh A, Vaziri F, Tabrizi F, et al. A systems medicine approach reveals disordered immune system and lipid metabolism in multiple sclerosis patients. Clin Exp Immunol. 2018;192(1):18-32.
36. Loor JJ, Dann HM, Everts RE, Oliveira R, Green CA, Guretzky NA, et al. Temporal gene expression profiling of liver from periparturient dairy cows reveals complex adaptive mechanisms in hepatic function. Physiol Genomics. 2005; 23(2):217-226.
37. Rodriguez, Montserrat A. De La Rosa, and S. Kersten. Regulation of lipid droplet-associated proteins by peroxisome proliferator-activated receptors. Biochim Biophys Acta Mol Cell Biol Lipids. 2017; 1862(10 Pt B):1212-1220.
38. He YH, He Y, Liao XL, Niu YC, Wang G, Zhao C, et al. The calcium-sensing receptor promotes adipocyte differentiation and adipogenesis through PPARγ pathway. Mol Cell Biochem. 2012; 361(1-2):321-328.
39. Han H, Cao A, Wang L, Guo H, Zang Y, Li Z, et al. Huangqi Decoction Ameliorates Streptozotocin-Induced Rat Diabetic Nephropathy through Antioxidant and Regulation of the TGF-β/MAPK/PPAR-γ Signaling. Cell Physiol Biochem. 2017; 42(5):1934-1944.
40. Agarwal S, Chattopadhyay M, Mukherjee S, Dasgupta S, Mukhopadhyay S, Bhattacharya S. Fetuin-A downregulates adiponectin through Wnt-PPARγ pathway in lipid induced inflamed adipocyte. Biochim Biophys Acta Mol Basis Dis. 2017; 1863(1):174-181.
41. Huan-Xian Cui, Ran-Ran Liu, Gui-Ping Zhao, Mai-Qing Zheng, Ji-Lan Chen, Jie Wen. Identification of differentially expressed genes and pathways for intramuscular fat deposition in pectoralis major tissues of fast-and slow-growing chickens. BMC Genomics. 2012; 13:213.
42. Mortazavi A, Williams BA, McCue K, Schaeffer L, Wold B. Mapping and quantifying mammalian transcriptomes by RNA-Seq. Nature Methods. 2008; 5: 621.

43. Kanehisa M, Goto S. KEGG: Kyoto Encyclopedia of Genes and Genomes. Nucleic Acids Research. 1999; 28(1): 27-30.
44. Livak KJ, Schmittgen TD. Analysis of Relative Gene Expression Data Using Real-Time Quantitative PCR and the $2^{-\Delta\Delta CT}$ Method. Methods-A Companion To Methods in Enzymology. 2001; 25 (4):402-408.

Figures

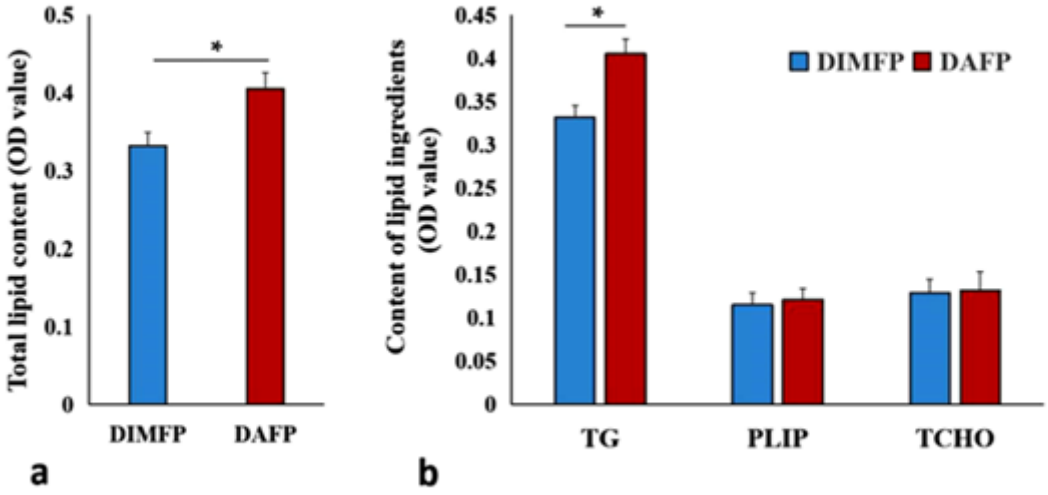

Figure 1

The difference of lipid metabolism between DIMFPs and DAFPs of chicken. (a) and (b) The contents of total lipid and the main ingredient of lipid (TG, PLIP and TCHO). The content of total lipid and TG were increased in the DAFPs than in the DIMFP after two days with 100% confluence. Data are presented as means ± SEM ($n = 3$; * $P < 0.05$);

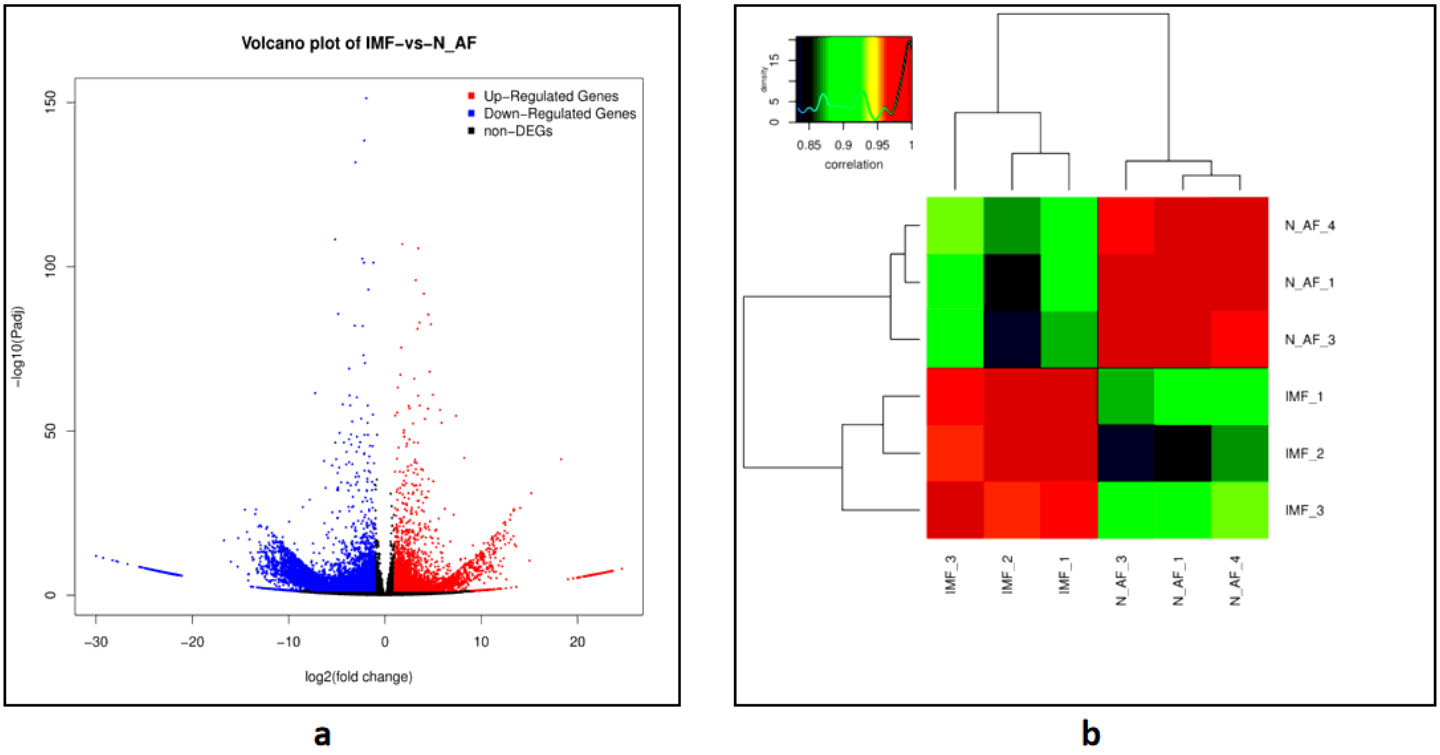

Figure 2

Volcano plot and cluster analysis of differentially expressed genes (DEGs). (a) Volcano plot. Red dots (UP) represent significantly up-regulated genes (log2FC ≥ 1.0, FDR < 0.05); green dots (DOWN) represent significantly down-regulated genes (log2 FC ≤ −1.0, FDR < 0.05); black dots (NO) represent DEGs below the level of significance; (b) based on 3486 known DEGs in DIMFP and DAFP of chickens, the cluster analysis was performed. The results show that the data in the gene expression profiling in same group were closely related.

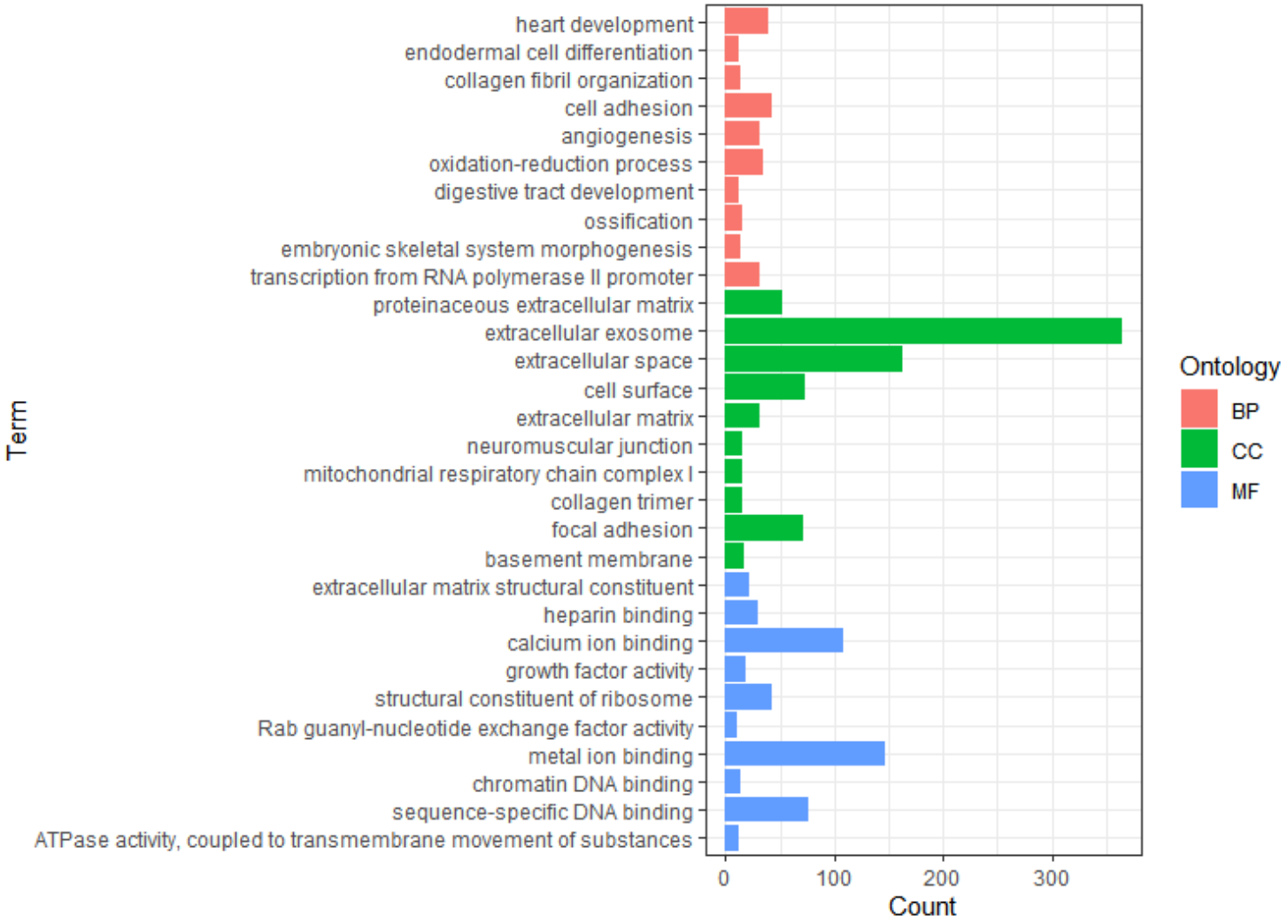

Figure 3

The list of enriched Gene Ontology (GO) terms with top 10. The enriched Gene Ontology (GO) terms were enriched (P <0.05) based on the 3486 DEGs, and the GO terms with top 10 of biological process (BP), cellular component (CC) and molecular function (MF) were listed.

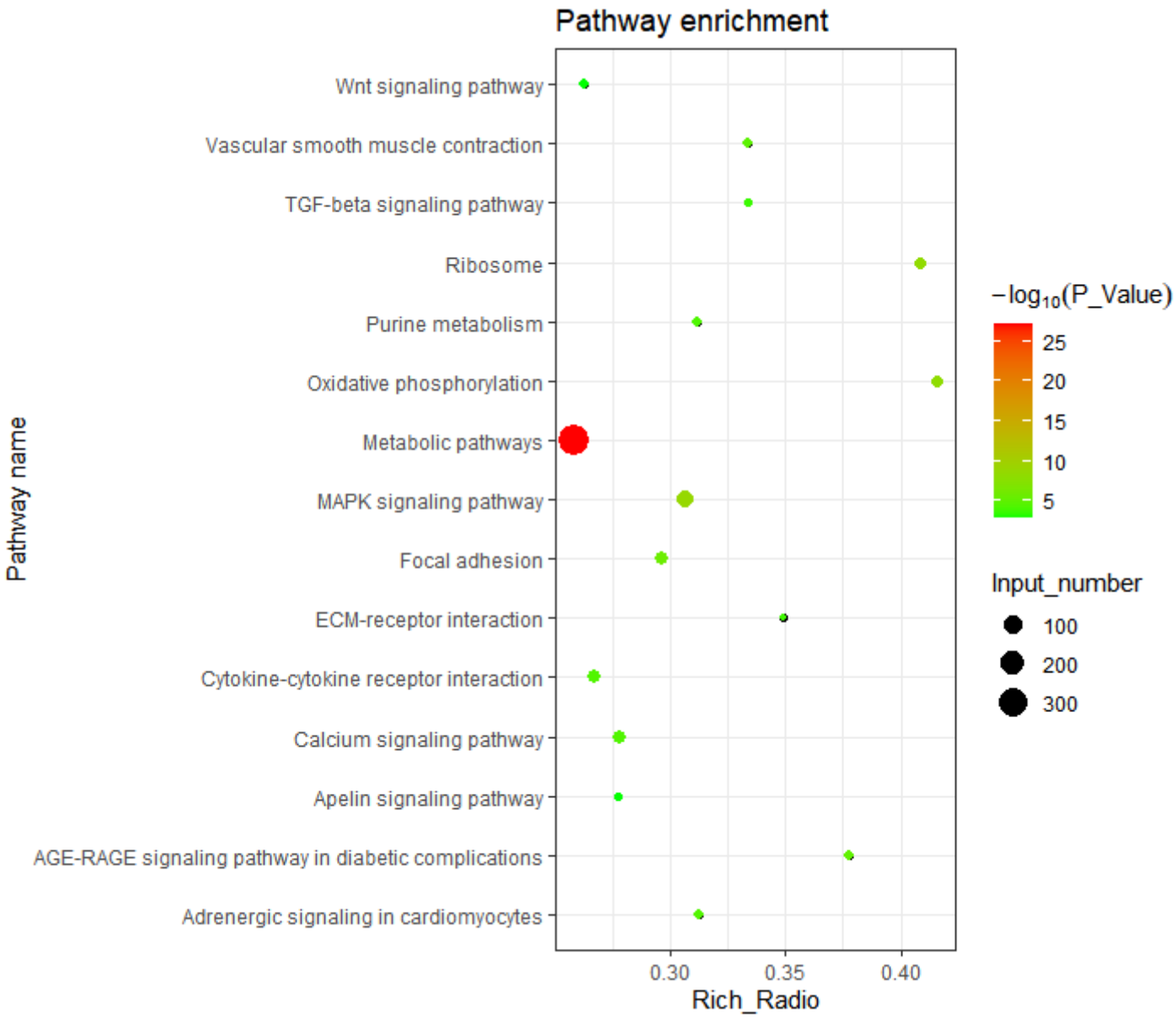

Figure 4

The list of enriched pathways with top 15 based on the 3486 DEGs. The KEGG (Kyoto Encyclopedia of Genes and Genomes) pathway analysis showed that well-known pathways (MAPK-, TGF beta-, Wnt-, Calcium-, PPAR signaling pathway) on lipid metabolism pathways were enriched, and the enriched pathways with top 15 were screen (adjusted $P < 0.05$).

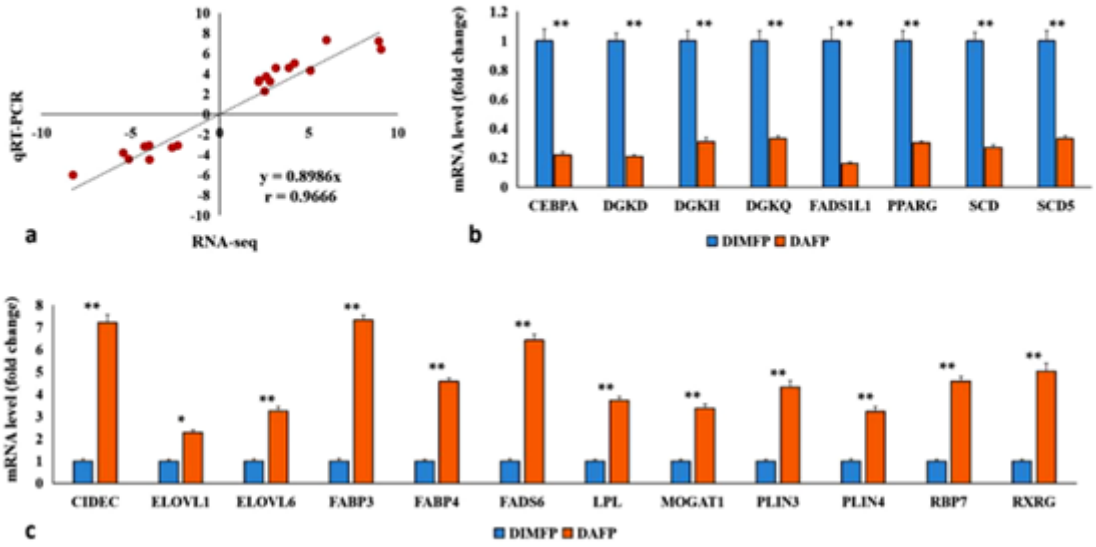

Figure 5

The validation of DEGs related to lipid metabolism between DIMFPs and DAFPs of chicken. (a) Correlation analysis of gene expression profiling and Real-time quantitative polymerase chain reaction (qRT-PCR) results by Spearman rank correlation in DIMFPs and DAFPs. A high correlation coefficient (r =0.9666, P < 0.05) was detected, which indicates that the gene expression profiling data are reliable. n = 20; (b) and (c) The qRT-PCR verification of DEGs detected by gene expression profiling. The expression levels of DEGs related to lipid metabolism determined by qRT-PCR in the DIMFPs and DAFPs. Each of these DEGs were up-regulated or down-regulated significantly (P < 0.05) in DIMFPs and DAFPs. Data are presented as means ± SEM (n = 3; * P < 0.05, ** P < 0.01);

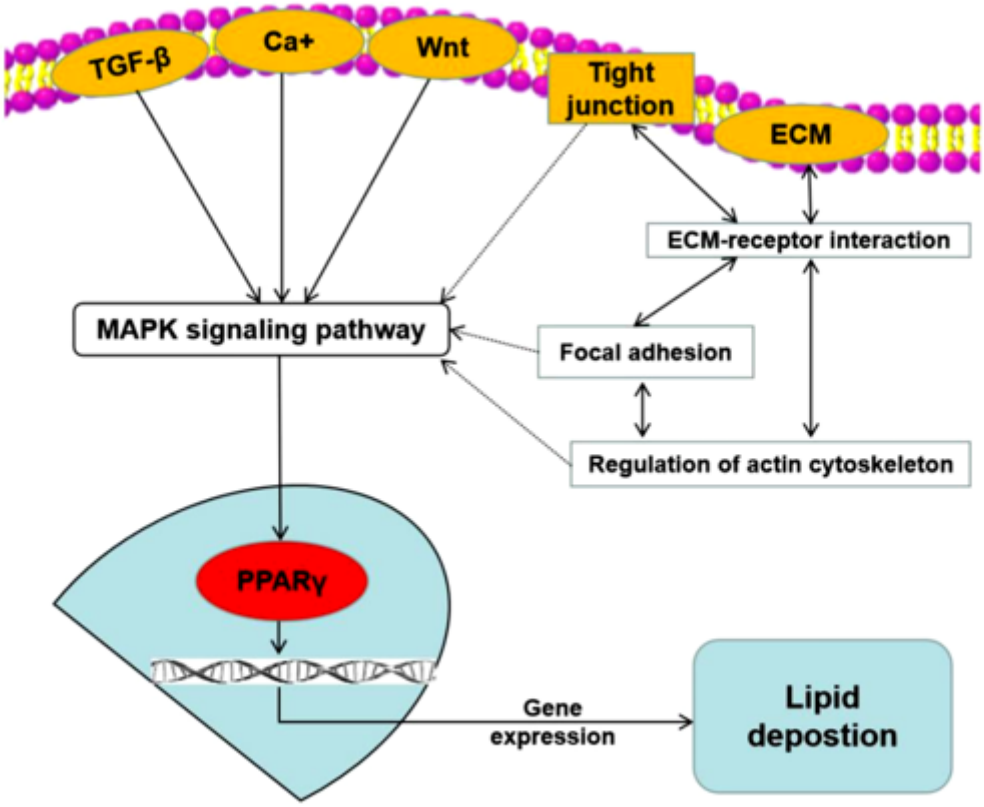

Figure 6

The proposed regulatory network on the difference of lipid deposition DIMFPs and DAFPs based on DEGs and enriched signaling pathways.

Supplementary Files

This is a list of supplementary files associated with this preprint. Click to download.

- Additionalfile1TableS1.xls
- Additionalfile2TableS2.xlsx
- Additionalfile3TableS3.xls
- Additionalfile4TableS4.xls
- Additionalfile5TableS5.xls
- Additionalfile6TableS6.xls
- Additionalfile7FigureS1.png
- Additionalfile8FigureS2.png
- Additionalfile9FigureS3.png
- Additionalfile10FigureS4.png

- Additionalfile11KEGGPERMISSION.pdf